Chemical Science

ROYAL SOCIETY OF CHEMISTRY

EDGE ARTICLE

View Article Online
View Journal | View Issue

Cite this: *Chem. Sci.*, 2025, **16**, 16151

All publication charges for this article have been paid for by the Royal Society of Chemistry

Near-infrared light-activated *Z*-to-*E* isomerization of azobenzene *via* triplet sensitization from PbS quantum dots

Yanan Feng,[a] Qingxin Luan,[a] Shuai Zhang,[a] Lin Xi,[a] Shijie Zhang,[a] Kezhou Chen,[a] Tiegen Liu[a] and Lili Hou *[ab]

Received 22nd May 2025
Accepted 30th July 2025

DOI: 10.1039/d5sc03719k

rsc.li/chemical-science

Azobenzene (**Azo**) photoswitches have attracted significant attention for developing smart photoresponsive materials owing to their reversible light-induced isomerization between *E* and *Z* configurations. However, it is challenging to design an **Azo** capable of quantitative and efficient *Z* → *E* photoisomerization under low-energy photon irradiation, particularly near-infrared (NIR) light above 800 nm. Here, we demonstrate that *Z* → *E* photoswitching of **Azo** can be achieved under 808 nm light irradiation when PbS quantum dots (QDs) are combined with carboxylated **Azo** (**Azo1**). The unique spin–orbit coupling of PbS QDs facilitates efficient triplet energy transfer to *Z*-**Azo1** under NIR light irradiation, thereby facilitating *Z* → *E* photoswitching *via* the excited triplet surface. Importantly, the broad absorption spectrum of PbS QDs enables activation of *Z* → *E* photoisomerization using any desired wavelength across the visible and NIR spectra up to 900 nm. The photoswitching of **Azo1** when combined with PbS QDs exhibits reversible photoisomerization and good fatigue resistance over alternating irradiation cycles of 365 nm and 808 nm light. Our strategy of combining **Azo** and QDs holds promise for advancing the development of high-performance NIR light-activated optoelectronic materials and devices.

Introduction

Azobenzenes (**Azo**), as one of the most commonly used photoswitchable molecules, have garnered significant attention in designing smart materials,[1,2] optoelectronic devices,[3,4] solar energy storage,[5,6] photomechanical actuation,[7,8] and biological sciences,[9,10] due to their pronounced photochromic properties arising from reversible *E* and *Z* geometric isomerisms.[11,12] The *E* isomer of parent **Azo** exhibits a strong π → π* absorbance band around 320 nm, and ultraviolet (UV) light irradiation can induce *E* → *Z* photoisomerization.[13] The *Z* isomer displays a prominent n → π* band centered at approximately 440 nm and is highly responsive to purple/blue light irradiation.[14] In addition, other stimulations such as heat,[15] acid,[16] redox,[17] catalysts,[18] electric field,[19] *etc.*, can also facilitate the reverse *Z* → *E* isomerization.[20,21] Owing to the isomerization *via* the first triplet excited state (T_1), which strongly favors the *E*-**Azo** form and exhibits considerable spin–orbit coupling,[22,23] the *Z* → *E* photoisomerization process of **Azo** can be activated through triplet energy transfer (TET) from sensitizers by indirect excitation using low-energy, long-wavelength light.[24,25] This can minimize the photodamage and deepen tissue penetration, making it particularly attractive for applications such as deep-tissue optogenetics, high-resolution bioimaging, and photopharmacology.[26–28] Transition metal complexes (such as Pt^{II},[29] Pb^{II},[30] *etc.*) are generally employed as triplet sensitizers, by which the *Z* → *E* photoisomerization of **Azo** derivatives can be efficiently activated through the TET process using green, yellow, or red light.[31,32] However, commonly used sensitizers feature limited absorption windows, low light absorptivity and restricted tunability of triplet state energies, and it's highly challenging to activate *Z* → *E* photoisomerization using near-infrared (NIR) light (>800 nm).

Colloidal semiconductor quantum dots (QDs), featuring broadband absorption, high absorption cross-sections, size-tunable bandgaps and photoluminescence (PL) due to the strong quantum confinement effect,[33–35] have been widely applied in bioimaging,[36] displays and lighting,[37] and quantum information processing.[38] Importantly, the strong spin–orbit coupling in QDs mixes singlet and triplet characteristics, which can promote the transfer of triplet excitons from QDs to surface-anchored molecules *via* highly efficient TET.[39–41] Therefore, QDs have also been employed in a range of important triplet excited state related transformations, such as photochemical cycloaddition reactions,[42] and triplet–triplet annihilation photon upconversion.[43] Recently, we have successfully achieved visible light-induced photocyclization of photoswitchable

[a]*State Key Laboratory of Precision Measurement Technology and Instruments, Key Laboratory of Opto-electronics Information Technology, School of Precision Instrument and Opto-Electronics Engineering, Tianjin University, Tianjin 300072, China. E-mail: lilihou@tju.edu.cn*

[b]*Department of Chemistry and Chemical Engineering, Chalmers University of Technology, Gothenburg, Sweden*

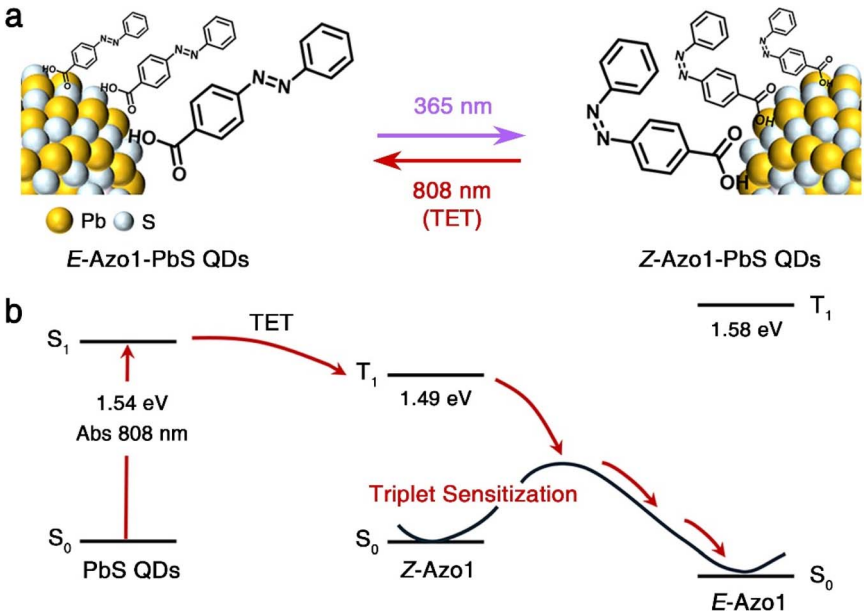

Scheme 1 (a) Schematic illustration of *Z*–*E* photoisomerization of PbS QDs and carboxylated **Azo1** under UV and NIR light irradiation. (b) Energetical diagram of the TET from PbS QDs to *Z*-**Azo1** for activating *Z* → *E* photoisomerization under 808 nm light irradiation.

diarylethenes through TET using CdS QDs.[44,45] Although the design of QD-sensitized **Azo** photoswitches offers a promising strategy for activating *Z* → *E* photoisomerization using long-wavelength light, especially in the NIR region, it remains a largely unexplored area.

Herein, NIR light-activated *Z* → *E* photoisomerization of a carboxylated **Azo** (**Azo1**) photoswitch is developed based on PbS QDs through the TET process under 808 nm excitation (Scheme 1). In our design, **Azo1** can dynamically anchor onto the surface of PbS QDs *via* coordination bonds of its carboxyl functional groups, which allows efficient triplet sensitization. Upon irradiation with 808 nm NIR light, the excited state PbS QDs act as triplet sensitizers, undergoing TET to *Z*-**Azo1** to initiate *Z* → *E* photoisomerization. The photoswitching process demonstrates efficient isomerization, showing good reversibility with a conversion yield of up to 100%. Importantly, compared to previously reported approaches using molecular sensitizers with limited absorption bands, the broad absorption region of PbS QDs across the entire visible and part of the NIR band enables active *Z* → *E* photoisomerization of **Azo1** using any desired color light. This NIR QD-activated triplet sensitization strategy not only opens new possibilities for the design of efficient photoresponsive materials but also paves the way for the development of high-performance NIR light-activated optoelectronic materials and devices.

Results and discussion

Materials and characterization

PbS QDs were synthesized according to a previous report.[46] The absorption and PL spectra of PbS QDs in toluene are shown in Fig. 1a. PbS QDs exhibit a broad absorption spectrum from 300 nm to 900 nm, with the first exciton absorption band located in the NIR region (peak around 808 nm). The emission peak of PbS QDs is centered at 900 nm when excited at 760 nm. Transmission electron microscopy (TEM) indicates that these PbS QDs have a highly monodisperse and uniform morphology (the inset of Fig. 1a) with an average diameter of 2.75 nm (Fig. S1a). The main X-ray diffraction (XRD) peaks (Fig. S1b) can be ascribed to the standard cubic phase of PbS QDs (PDF #05-0592), confirming the high quality of synthesized PbS QDs. Fig. 1b shows the absorption spectra and corresponding molecular configurations of *E*-**Azo1** and *Z*-**Azo1** isomers. Upon irradiation with 365 nm light (137 mW cm^{-2} for 30 s), *E* → *Z* photoisomerization occurs, resulting in a significant decrease in the absorption band peaking at 324 nm and a slight increase in the visible band centered at 445 nm. The photostationary state (PSS) upon exposure to 365 nm light consists of 34% *E*-**Azo1** and 66% *Z*-**Azo1**.[47] Subsequently, irradiation with 450 nm light (126 mW cm^{-2} for 20 s) induces the reverse *Z* → *E* photoisomerization, and the absorption spectrum fully recovers to the initial state. **Azo1** exhibits a half-life of 16.9 h in toluene at 28 °C for *Z* → *E* thermal isomerization (Fig. S2a). These observations demonstrate that *E*-**Azo1** and *Z*-**Azo1** isomers can reversibly interconvert upon alternating exposure to UV and blue light.

NIR light-activated *Z* → *E* photoisomerization

To demonstrate the NIR light-activated *Z* → *E* photoisomerization of **Azo1**, a mixed solution containing 0.2 μM PbS QDs and 100 μM **Azo1** was prepared in deaerated toluene and the absorption spectra are shown in Fig. 2a. Due to the high molar absorption coefficient of PbS QDs, $\varepsilon_{808\ nm} = 3.79 \times 10^4$ cm^{-1} M^{-1}, only a small amount of sensitizer is required compared to the organic sensitizers paired with **Azo** photoswitches reported previously.[48,49] By comparing the absorption

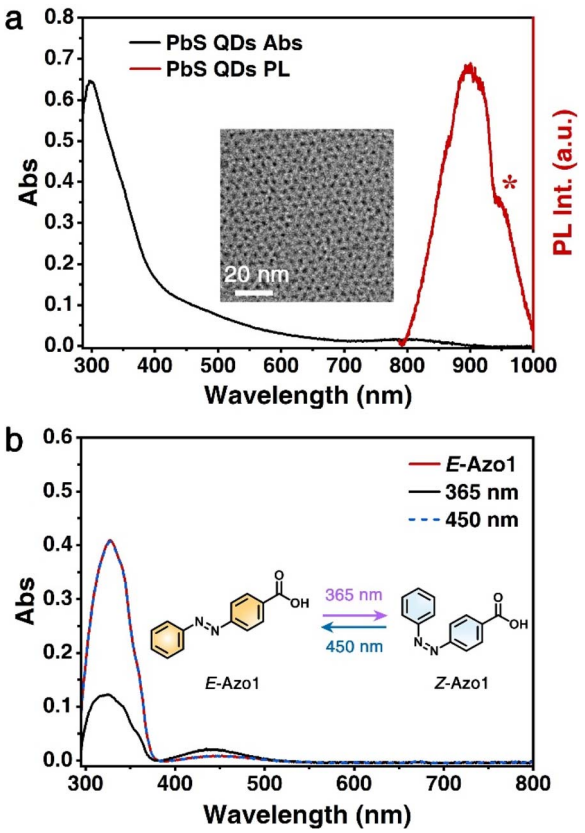

Fig. 1 Optical properties of PbS QDs and **Azo1**. (a) Absorption and PL spectra of PbS QDs (0.1 μM) in toluene, and (inset) TEM image of PbS QDs. *The distortion of the Gaussian band shape is caused by the artefact of the spectrometer. (b) Absorption spectra of *E*-**Azo1** (50 μM) in toluene as well as after 365 nm and 450 nm light irradiation. The inset chemical structures illustrate *E*–*Z* reversible photoisomerization upon 365 nm and 450 nm light irradiation.

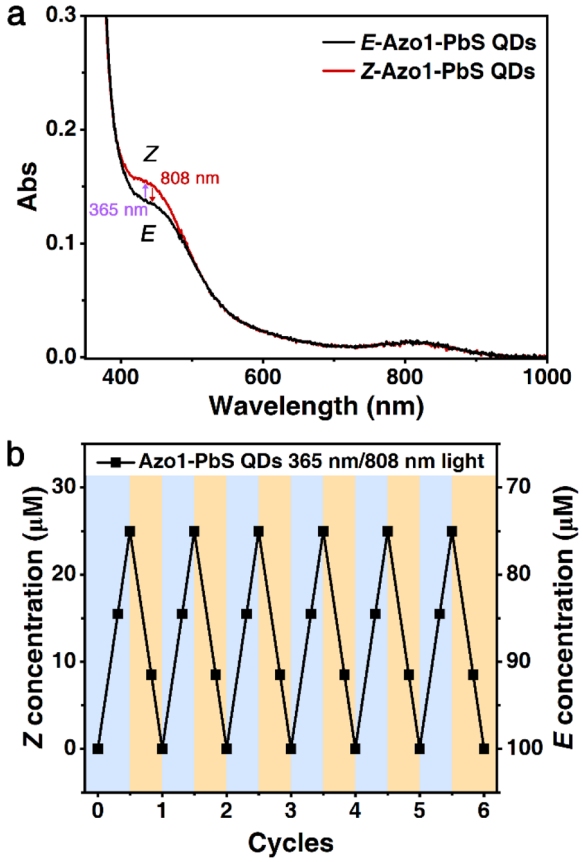

Fig. 2 Photoisomerization of the absorption spectra of PbS QDs (0.2 μM) mixed with **Azo1** (100 μM). (a) Absorption spectra of the mixed solution after 365 nm (30 s) and 808 nm (50 s) light irradiation. (b) Reversible *E*–*Z* photoisomerization of the mixed solution was monitored by *E*/*Z* isomer concentration under alternating 365 nm (5 s, 30 s) and 808 nm (10 s, 50 s) light irradiation.

spectra of **Azo1** with or without PbS QDs (Fig. S3), no obvious spectral shift is observed for **Azo1** in the presence of PbS QDs, indicating no or very weak interaction between **Azo1** and PbS QDs at the ground state. This is unlike previously reported cases of thiol-functionalized **Azo** attached to the surface of $CuInS_2$ QDs, where the newly formed species underwent different photoisomerization processes than those of parent **Azo**.[50] When mixed with PbS QDs, **Azo1** possesses a half-life of 13.6 h in toluene at 28 °C for $Z \rightarrow E$ thermal isomerization (Fig. S2b), which is slightly shorter than that of **Azo1** alone, possibly due to changes in the dielectric and coordination environment near the PbS QD surface.

The $E \rightarrow Z$ photoisomerization of **Azo1** occurs as parent **Azo** in our mixed solution, as evidenced by the increased absorption band between 400 nm and 500 nm upon 365 nm light excitation. Remarkably, upon subsequent irradiation with 808 nm light (1.94 W cm^{-2} for 50 s), the raised absorption band decreases to its initial state. This change is identical to that under 450 nm light irradiation (Fig. S4), confirming that $Z \rightarrow E$ photoisomerization can be activated using NIR light in the presence of PbS QDs. Notably, 808 nm excitation exhibits a significantly stronger bias toward $Z \rightarrow E$ photoisomerization compared to 365 nm, where *E*-**Azo1** absorbs and can undergo back conversion. Thanks to the broad absorption spectrum of PbS QDs, it allows us to activate $Z \rightarrow E$ photoisomerization of **Azo1** using not only the NIR light but also any desired wavelength across the entire visible spectrum. Particularly, green (550 nm), yellow (590 nm), deep-red (760 nm), and white light with a 550 nm long-pass filter are also employed to activate $Z \rightarrow E$ photoisomerization. The absorption spectra of *Z*-**Azo1** under these visible light irradiations all show a gradual decrease between 400 nm and 500 nm, confirming a quantitative conversion (100%) from *Z*-**Azo1** to *E*-**Azo1** when mixed with PbS QDs (Fig. S5).

To systematically evaluate the photoisomerization process of **Azo1** mixed with PbS QDs, the conversion at the PSS and the photoisomerization quantum yield (QY) of **Azo1** were determined. After 365 nm light irradiation, a lower conversion from *E*-to-*Z* isomers was observed in the presence of PbS QDs, with 25% of *Z*-**Azo1** and 75% of *E*-**Azo1**. The QY of **Azo1** in the presence of PbS QDs under 365 nm light irradiation is determined to be 0.04, which is also lower than that of **Azo1** alone (0.12) (Table S1). The reduced conversion and QY under UV light irradiation may be attributed to: (1) the strong absorption of PbS QDs, which attenuates the incident UV light available for

E-**Azo1** excitation, and (2) the promotion of the reverse $Z \rightarrow E$ isomerization *via* the TET process from PbS QDs. Moreover, to further explore the wavelength-dependent $Z \rightarrow E$ photoisomerization efficiency of **Azo1** mixed with PbS QDs, the photoisomerization QYs of **Azo1** under 450 nm, 515 nm, 550 nm, and 590 nm light irradiation were determined by using Aberchrome **670** actinometry (see the ESI for more details and Table S2), and an action plot[51] was constructed as shown in Fig. S6. When the excitation wavelength red-shifts, the photoisomerization QY of **Azo1** improves from 0.13 (under 515 nm excitation) to 0.20 (under 590 nm excitation). **Azo1** exhibits a relatively high QY of 0.17 under 450 nm excitation, which originates from photons absorbed directly by *Z*-**Azo1** and sensitized from PbS QDs *via* the TET process.

To investigate the reversibility and fatigue resistance of the **Azo1**-PbS QD system, the changes of *E*/*Z* isomer concentrations were monitored over six cycles under alternating 365 nm and 808 nm light irradiation (Fig. 2b). There is no discernible photoswitching fatigue observed, and the photoisomerization rate remains the same under irradiation cycles. It should be noted that PbS QDs alone, under cycled light irradiation, do not exhibit any photoswitching behavior (Fig. S7). It demonstrates that our approach of combining **Azo1** with PbS QDs can effectively and reversibly activate $Z \rightarrow E$ photoisomerization using NIR light and exhibits good fatigue resistance.

Mechanistic investigation of triplet sensitization

Our design to achieve NIR light-activated $Z \rightarrow E$ photoisomerization relies on the unique TET from PbS QDs *via* short-range Dexter-type energy transfer (a few nanometers).[52–54] Therefore, close proximity between PbS QDs and **Azo1** is required, with the carboxyl functional groups of **Azo1** anchoring onto the surface of PbS QDs. The T_1 of *Z*-**Azo1** was calculated to be 1.49 eV (see computational details in the ESI and Table S3), which is lower than that of PbS QDs (~1.54 eV, estimated from the first excitonic absorption band).[55] Consequently, the TET from PbS QDs to the *Z*-**Azo1** isomer allows for a more efficient process than that of the *E*-**Azo1** isomer, whose T_1 is slightly higher than that of PbS QDs, as indicated in Scheme 1b. We compared the $Z \rightarrow E$ photoisomerization of carboxylic acid-substituted **Azo1** and unsubstituted parent **Azo** in the presence of PbS QDs. Fig. 3a shows the changes in the absorption spectra of the mixed solution of PbS QDs and **Azo1** (66% *Z*, 34% *E*) under 808 nm light irradiation at different time intervals, and the kinetics monitored at 445 nm over time are presented in Fig. 3b. Under 808 nm light irradiation, 100% *E*-isomer of **Azo1** is generated within 100 s (Fig. 3b, black triangles). In contrast, the unsubstituted parent *Z*-**Azo** exhibits no changes in the absorbance under the same irradiation conditions (Fig. 3b, blue circles). *Z*-**Azo1** alone under 808 nm light irradiation also exhibits no changes in its absorption spectrum (Fig. S8), which can rule out NIR-induced heating effects that contribute to the *Z*-to-*E* isomerization. Therefore, it demonstrates that the efficient TET process is the key mechanism to activate $Z \rightarrow E$ photoisomerization, which only occurs when the **Azo** moiety has the capability of anchoring onto the surface of PbS QDs.

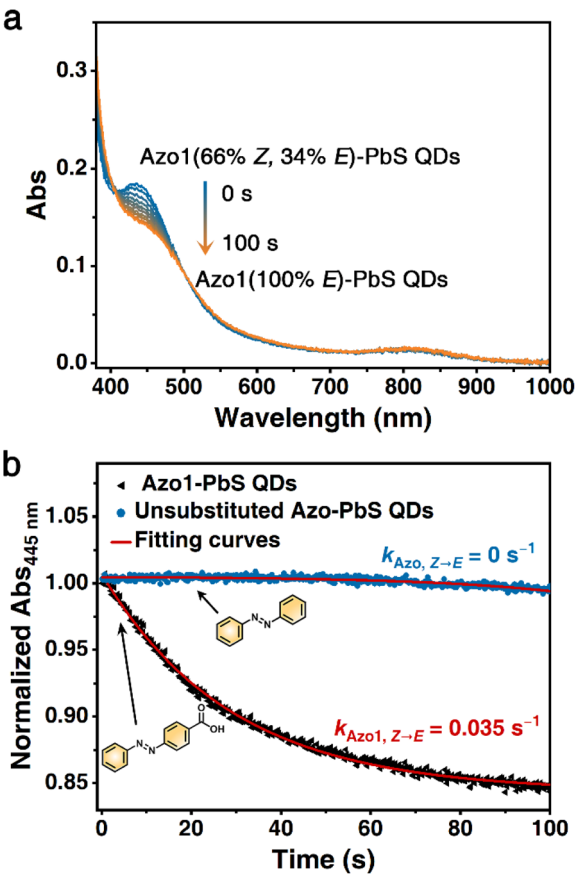

Fig. 3 Triplet sensitized $Z \rightarrow E$ photoisomerization kinetics. (a) Absorption spectra of the mixed solution of 0.2 μM PbS QDs and 100 μM **Azo1** (66 μM *Z*-**Azo1** and 34 μM *E*-**Azo1**) under 808 nm light irradiation over time. (b) The time-dependent $Z \rightarrow E$ photoisomerization of PbS QDs with *Z*-**Azo1** and with unsubstituted *Z*-**Azo** was monitored by the absorbance at 445 nm.

To further investigate the TET mechanism from PbS QDs to **Azo1**, steady-state and time-resolved PL spectra of PbS QDs were measured in the absence and presence of *Z*-**Azo1**. PbS QDs exhibit a maximum PL emission band centered at 900 nm, and the PL intensity shows significant quenching with the addition of *Z*-**Azo1** (Fig. 4a). The PL decay of PbS QDs indicates an amplitude-weighted average lifetime of 1.99 μs (Table S4), and the PL lifetime also demonstrates pronounced quenching upon introduction of *Z*-**Azo1** (Fig. 4b). Specifically, when the concentration ratio of PbS QDs to *Z*-**Azo1** reaches 1 : 100, the PL lifetime decreases to 0.677 μs. These results clearly indicate that efficient energy transfer occurs from PbS QDs to *Z*-**Azo1**.

Stern–Volmer quenching analysis was performed to evaluate both the PL intensity and lifetime, respectively (Fig. 4c and d). The bimolecular quenching rate constants (k_q), obtained from the linear fit of the Stern–Volmer plot, are 3.52×10^9 L mol^{-1} s^{-1} for PL intensity and 4.75×10^9 L mol^{-1} s^{-1} for PL lifetime, respectively, which are within the expected range for a diffusion-controlled process. The PL quenching of PbS QDs by *E*-**Azo1** was also performed for comparison (Fig. S9). As expected, less efficient quenching occurs with reduced quenching rate constants

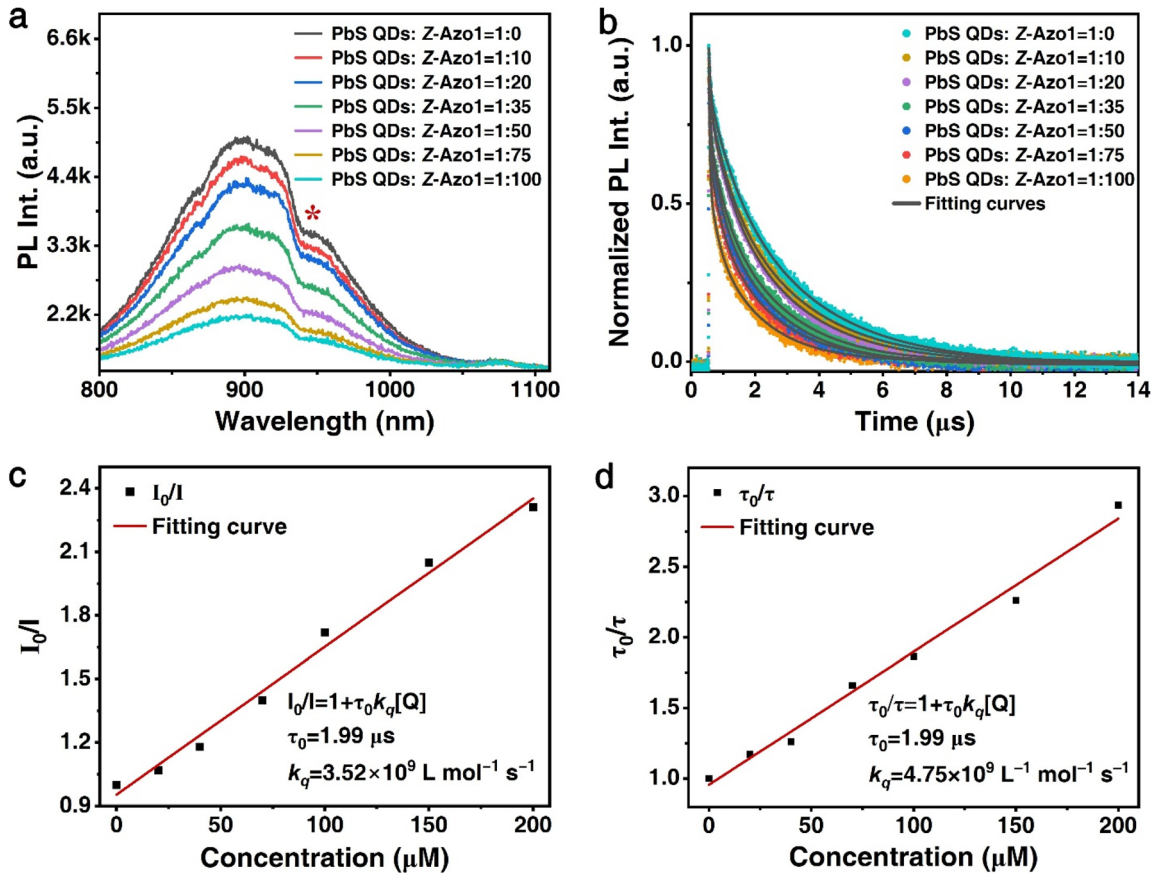

Fig. 4 PL quenching of PbS QDs by adding *Z*-**Azo1**. (a) PL spectra under 760 nm excitation and (b) time-resolved PL decay at 880 nm under 600 nm pulsed excitation of PbS QDs (2 μM) without and with *Z*-**Azo1** (20, 40, 70, 100, 150, 200 μM) in toluene. *The distortion of the Gaussian band shape is caused by the artefact in the spectrometer. Stern–Volmer plots and linear fits for (c) PL and (d) PL lifetime quenching PbS QDs by *Z*-**Azo1**.

obtained for both PL intensity and lifetime. TET from PbS QDs to *E*-**Azo1** may also occur *via* an endogenic process, which results in lower *Z*-to-*E* QYs through triplet sensitization, compared to that under direct 450 nm light irradiation.

Ultrafast transient absorption spectroscopy was performed to further investigate the mechanism of PbS QD-sensitized *Z*-**Azo1** photoisomerization (Fig. S10 and S11). The femtosecond transient absorption (fsTA) spectrum of PbS QDs shows a characteristic exciton bleach around 800 nm, which is consistent with previously reported PbS QDs.[56] Upon introduction of *Z*-**Azo1**, the transient feature of PbS QDs remains unchanged, and the bleaching lifetime within 7 ns is almost the same as that of only PbS QDs (Fig. S10). The nanosecond transient absorption (nsTA) spectrum of PbS QDs also exhibits an exciton bleach feature around 800 nm and the lifetime is determined to be 2.08 μs. When mixed with *Z*-**Azo1**, the exciton bleach of PbS QDs is accelerated with a faster recovery of lifetime (1.49 μs). Notably, no new spectral features are observed either in the fsTA or nsTA spectra, indicating the absence of significant electron transfer from PbS QDs to *Z*-**Azo1**. Förster resonance energy transfer (FRET) can be ruled out in this system, as there is no overlap between the absorption spectra of either form of **Azo1** and the PL spectrum of PbS QDs. As no transient triplet absorption of **Azo** has been observed experimentally,[57,58] previous reports indicate that the PL quenching of PbS QDs is primarily due to TET occurring from the QDs to the organic molecules.[59,60] Therefore, we conclude that the TET is the main mechanism responsible for PbS QD activated *Z*-**Azo1** photoisomerization.

Conclusions

In conclusion, we have developed a NIR light-activated **Azo** photoswitch based on PbS QDs. Under 808 nm light irradiation, a 100% conversion of $Z \rightarrow E$ photoisomerization of **Azo1** is achieved *via* TET from PbS QDs. The photoswitching process exhibits good fatigue resistance over multiple irradiation cycles. PbS QDs represent excellent candidates for activating $Z \rightarrow E$ photoisomerization due to their high molar absorption coefficient, size-tunable energy levels, and efficient TET capability. Moreover, benefiting from the broadband absorption of PbS QDs, quantitative $Z \rightarrow E$ photoisomerization of **Azo1** can be activated using any desired wavelength across the visible and NIR spectra up to 900 nm, representing the longest activation wavelength for TET-based **Azo** photoswitches to date. PL quenching and transient absorption spectroscopy studies confirm the mechanism of efficient TET from PbS QDs to **Azo1**.

Our future efforts will be directed to explore PbS QDs with varied sizes to activate **Azo** derivatives and investigate their NIR light-induced photochemical properties. This NIR light-activated photoswitching strategy holds promise for advancing next-generation photoresponsive materials and devices.

Author contributions

L. H. conceived the concept and supervised the research. L. H. and Y. F. designed the project. Y. F. and L. X. carried out material synthesis. Y. F. and Q. L. performed material characterization tests. S. Z did DFT calculations. Y. F. and L. H. wrote the paper. S. Z., K. C., and T. L. gave advice on the research. All authors discussed the results and commented on the manuscript.

Conflicts of interest

There are no conflicts to declare.

Data availability

The data supporting this article have been included as part of the SI.

SI is available: methods, experiments, computational details and additional spectra. See DOI: **https://doi.org/10.1039/d5sc03719k**.

Acknowledgements

L. H. acknowledges support from the Key Technologies Research and Development Program of China (2023YFB3609300) and National Natural Science Foundation of China (12274320 and 62205240).

Notes and references

1 D. Sharma, S. P. Rath, B. Kundu, A. Korkmaz, H. S, D. Thompson, N. Bhat, S. Goswami, R. S. Williams and S. Goswami, *Nature*, 2024, **633**, 560–566.
2 M. Ovalle, D. Doellerer and B. L. Feringa, *Angew. Chem., Int. Ed.*, 2025, **64**, e202501872.
3 Y. Kim, H. Bark, A. Gupta, Y. Zhang, J. Lee and P. S. Lee, *Adv. Energy Mater.*, 2025, **15**, 2405480.
4 F. Corrado, U. Bruno, M. Prato, A. Carella, V. Criscuolo, A. Massaro, M. Pavone, A. B. Muñoz-García, S. Forti, C. Coletti, O. Bettucci and F. Santoro, *Nat. Commun.*, 2023, **14**, 6760.
5 Z. Zhang, D. Dong, T. Bösking, T. Dang, C. Liu, W. Sun, M. Xie, S. Hecht and T. Li, *Angew. Chem., Int. Ed.*, 2024, **63**, e202404528.
6 Z. Wang, P. Erhart, T. Li, Z. Zhang, D. Sampedro, Z. Hu, H. A. Wegner, O. Brummel, J. Libuda, M. B. Nielsen and K. Moth-Poulsen, *Joule*, 2021, **5**, 3116–3136.
7 A. H. Gelebart, D. J. Mulder, M. Varga, A. Konya, G. Vantomme, E. W. Meijer, R. L. B. Selinger and D. J. Broer, *Nature*, 2017, **546**, 632–636.
8 Y. Li, B. Xue, J. Yang, J. Jiang, J. Liu, Y. Zhou, J. Zhang, M. Wu, Y. Yuan, Z. Zhu, Z. J. Wang, Y. Chen, Y. Harabuchi, T. Nakajima, W. Wang, S. Maeda, J. P. Gong and Y. Cao, *Nat. Chem.*, 2024, **16**, 446–455.
9 J. Gemen, J. R. Church, T.-P. Ruoko, N. Durandin, M. J. Białek, M. Weißenfels, M. Feller, M. Kazes, M. Odaybat, V. A. Borin, R. Kalepu, Y. Diskin-Posner, D. Oron, M. J. Fuchter, A. Priimagi, I. Schapiro and R. Klajn, *Science*, 2023, **381**, 1357–1363.
10 O. Bozovic, B. Jankovic and P. Hamm, *Nat. Rev. Chem.*, 2022, **6**, 112–124.
11 A. Mukherjee, M. D. Seyfried and B. J. Ravoo, *Angew. Chem., Int. Ed.*, 2023, **62**, e202304437.
12 H. Chen, W. Chen, Y. Lin, Y. Xie, S. Liu and J. Yin, *Chin. Chem. Lett.*, 2021, **32**, 2359–2368.
13 B. Tylkowski, A. Trojanowska, V. Marturano, M. Nowak, L. Marciniak, M. Giamberini, V. Ambrogi and P. Cerruti, *Coord. Chem. Rev.*, 2017, **351**, 205–217.
14 I. C. D. Merritt, D. Jacquemin and M. Vacher, *Phys. Chem. Chem. Phys.*, 2021, **23**, 19155–19165.
15 J. Garcia-Amorós, A. Sánchez-Ferrer, W. A. Massad, S. Nonell and D. Velasco, *Phys. Chem. Chem. Phys.*, 2010, **12**, 13238–13242.
16 A. Gibalova, L. Kortekaas, J. Simke and B. J. Ravoo, *Chem.–Eur. J.*, 2023, **29**, e202302215.
17 A. Goulet-Hanssens, C. Rietze, E. Titov, L. Abdullahu, L. Grubert, P. Saalfrank and S. Hecht, *Chem*, 2018, **4**, 1740–1755.
18 E. Titov, L. Lysyakova, N. Lomadze, A. V. Kabashin, P. Saalfrank and S. Santer, *J. Phys. Chem. C*, 2015, **119**, 17369–17377.
19 M. Alemani, M. V. Peters, S. Hecht, K.-H. Rieder, F. Moresco and L. Grill, *J. Am. Chem. Soc.*, 2006, **128**, 14446–14447.
20 B. Zhang, Y. Feng and W. Feng, *Nano-Micro Lett.*, 2022, **14**, 138.
21 S. Crespi, N. A. Simeth and B. König, *Nat. Rev. Chem.*, 2019, **3**, 133–146.
22 A. Cembran, F. Bernardi, M. Garavelli, L. Gagliardi and G. Orlandi, *J. Am. Chem. Soc.*, 2004, **126**, 3234–3243.
23 L. Gagliardi, G. Orlandi, F. Bernardi, A. Cembran and M. Garavelli, *Theor. Chem. Acc.*, 2004, **111**, 363–372.
24 F. A. Jerca, V. V. Jerca and R. Hoogenboom, *Nat. Rev. Chem.*, 2022, **6**, 51–69.
25 K. Kuntze, J. Isokuortti, J. J. van der Wal, T. Laaksonen, S. Crespi, N. A. Durandin and A. Priimagi, *Chem. Sci.*, 2024, **15**, 11684–11698.
26 H. Cheng, S. Zhang, J. Qi, X. Liang and J. Yoon, *Adv. Mater.*, 2021, **33**, 2007290.
27 M. Dong, A. Babalhavaeji, C. V. Collins, K. Jarrah, O. Sadovski, Q. Dai and G. A. Woolley, *J. Am. Chem. Soc.*, 2017, **139**, 13483–13486.
28 D. B. Konrad, G. Savasci, L. Allmendinger, D. Trauner, C. Ochsenfeld and A. M. Ali, *J. Am. Chem. Soc.*, 2020, **142**, 6538–6547.
29 J. Isokuortti, K. Kuntze, M. Virkki, Z. Ahmed, E. Vuorimaa-Laukkanen, M. A. Filatov, A. Turshatov, T. Laaksonen,

A. Priimagi and N. A. Durandin, *Chem. Sci.*, 2021, **12**, 7504–7509.
30 P. Bharmoria, S. Ghasemi, F. Edhborg, R. Losantos, Z. Wang, A. Mårtensson, M. Morikawa, N. Kimizuka, Ü. İşci, F. Dumoulin, B. Albinsson and K. Moth-Poulsen, *Chem. Sci.*, 2022, **13**, 11904–11911.
31 T. Dang, Z. Zhang and T. Li, *J. Am. Chem. Soc.*, 2024, **146**, 19609–19620.
32 Z. Wang, L. Fernandez, A. S. Aslam, M. Shamsabadi, L. M. Muhammad and K. Moth-Poulsen, *Responsive Mater.*, 2023, **1**, e20230012.
33 X. Zhang, H. Huang, C. Zhao and J. Yuan, *Chem. Soc. Rev.*, 2025, **54**, 3017–3060.
34 Q. Wu, F. Cao, W. Yu, S. Wang, W. Hou, Z. Lu, W. Cao, J. Zhang, X. Zhang, Y. Yang, G. Jia, J. Zhang and X. Yang, *Nature*, 2025, **639**, 633–639.
35 Z. Wang, Y. Gu, X. Li, Y. Liu, F. Liu and W. Wu, *Adv. Opt. Mater.*, 2023, **11**, 2300970.
36 K. D. Wegner and N. Hildebrandt, *TrAC, Trends Anal. Chem.*, 2024, **180**, 117922.
37 Y. Ren, X. Liang, X. Lu, B. Liu, L. Zhang, L. Zhang, Y. Huang, H. Zheng, Y. Jin and C. Liu, *Adv. Mater.*, 2025, **37**, 2417330.
38 H. Utzat, W. Sun, A. E. K. Kaplan, F. Krieg, M. Ginterseder, B. Spokoyny, N. D. Klein, K. E. Shulenberger, C. F. Perkinson, M. V. Kovalenko and M. G. Bawendi, *Science*, 2019, **363**, 1068–1072.
39 M. Liu, J. Zhu, G. Zhao, Y. Li, Y. Yang, K. Gao and K. Wu, *Nat. Mater.*, 2025, **24**, 260–267.
40 R. Lai, Y. Liu, X. Luo, L. Chen, Y. Han, M. Lv, G. Liang, J. Chen, C. Zhang, D. Di, G. D. Scholes, F. N. Castellano and K. Wu, *Nat. Commun.*, 2021, **12**, 1532.
41 G. Bao, R. Deng, D. Jin and X. Liu, *Nat. Rev. Mater.*, 2024, **10**, 28–43.
42 Y. Jiang, C. Wang, C. R. Rogers, M. S. Kodaimati and E. A. Weiss, *Nat. Chem.*, 2019, **11**, 1034–1040.
43 X. Lin, Z. Chen, Y. Han, C. Nie, P. Xia, S. He, J. Li and K. Wu, *ACS Energy Lett.*, 2022, **7**, 914–919.
44 K. Chen, J. Liu, J. Andréasson, B. Albinsson, T. Liu and L. Hou, *Chem. Sci.*, 2024, **15**, 20365–20370.
45 L. Hou, W. Larsson, S. Hecht, J. Andréasson and B. Albinsson, *J. Mater. Chem. C*, 2022, **10**, 15833–15842.
46 W. Huang, S. Wang, H. Gong, J. Tian, J. Peng and J. Cao, *Opt. Mater.*, 2023, **142**, 113977.
47 S. Neri, S. Garcia Martin, C. Pezzato and L. J. Prins, *J. Am. Chem. Soc.*, 2017, **139**, 1794–1797.
48 J. Isokuortti, T. Griebenow, J.-S. von Glasenapp, T. Raeker, M. A. Filatov, T. Laaksonen, R. Herges and N. A. Durandin, *Chem. Sci.*, 2023, **14**, 9161–9166.
49 M. Morikawa, M. Mizuno, N. Harada and N. Kimizuka, *Chem. Lett.*, 2023, **52**, 727–731.
50 Z. Ziani, C. Bellatreccia, F. P. Battaglia, G. Morselli, A. Gradone, P. Ceroni and M. Villa, *Nanoscale*, 2024, **16**, 12947–12956.
51 I. M. Irshadeen, S. L. Walden, M. Wegener, V. X. Truong, H. Frisch, J. P. Blinco and C. Barner-Kowollik, *J. Am. Chem. Soc.*, 2021, **143**, 21113–21126.
52 C. Mongin, S. Garakyaraghi, N. Razgoniaeva, M. Zamkov and F. N. Castellano, *Science*, 2016, **351**, 369–372.
53 Z. Zhang, W. Wang, M. O'Hagan, J. Dai, J. Zhang and H. Tian, *Angew. Chem., Int. Ed.*, 2022, **61**, e202205758.
54 W. Wang, W. Yang, Z. Zhang, J. Dai, Y. Xu and J. Zhang, *Chem. Sci.*, 2024, **15**, 5539–5547.
55 A. L. Efros, M. Rosen, M. Kuno, M. Nirmal, D. J. Norris and M. Bawendi, *Phys. Rev. B:Condens. Matter Mater. Phys.*, 1996, **54**, 4843–4856.
56 Z. Huang, Z. Xu, M. Mahboub, Z. Liang, P. Jaimes, P. Xia, K. R. Graham, M. L. Tang and T. Lian, *J. Am. Chem. Soc.*, 2019, **141**, 9769–9772.
57 H. M. D. Bandara and S. C. Burdette, *Chem. Soc. Rev.*, 2012, **41**, 1809–1825.
58 H. Rau, in *Photochromism: Molecules and Systems*, ed. H. Dürr and H. Bouas-Laurent, Elsevier, Amsterdam, 1990, ch. 4, vol. 1, pp. 165–192.
59 M. Wu, D. N. Congreve, M. W. B. Wilson, J. Jean, N. Geva, M. Welborn, T. Van Voorhis, V. Bulović, M. G. Bawendi and M. A. Baldo, *Nat. Photonics*, 2016, **10**, 31–34.
60 M. Mahboub, H. Maghsoudiganjeh, A. M. Pham, Z. Huang and M. L. Tang, *Adv. Funct. Mater.*, 2016, **26**, 6091–6097.